A Unified Tractography Framework for Comparing Diffusion Models on Clinical Scans

Christian Baumgartner[1], O. Michailovich[2], J. Levitt[1], O. Pasternak[1], S. Bouix[1], C-F Westin[1] and Yogesh Rathi[1]

[1] Brigham and Women's Hospital, Harvard Medical School, Boston,
[2] Department of Electrical Engg., University of Waterloo, Canada

Abstract. In this paper, we compare several parametric and non-parametric models of diffusion in a unified framework that allows simultaneous model estimation and tractography. The framework uses the Unscented Kalman Filter (UKF) to compare several variants of spherical harmonics (SH), i.e., SH with sharpening, spherical deconvolution, SH with solid angle and also several parametric models like single and two-tensor models with and without an additional "free water" component. We estimate all these models and perform tractography using the same optimizer, namely, the UKF. Comparison is done by tracing two fiber bundles whose connectivity is known from the literature on human anatomy. We trace these fiber bundles on 10 healthy subjects and compare how well each of these models perform on clinical in-vivo scans. For quantitative comparison, we propose two new measures; traceability and coverage, both of which capture how well each method performs in terms of tracing known fiber bundles. Our results show that, the two-tensor with "free-water" model performs very well for both these measures.

1 Introduction

Diffusion magnetic resonance imaging (dMRI) allows neuroscientists to investigate how neurons originating from one region connect to other regions, or how well-defined these connections may be. For such studies, the quality of the results relies heavily on the chosen fiber representation and the method of reconstructing pathways.

To begin studying the microstructure of fibers, we need a model to interpret the diffusion weighted signal. Such models fall broadly into two categories: parametric and nonparametric. One of the simplest parametric models is the diffusion tensor which describes a Gaussian estimate of the diffusion orientation and strength at each voxel. While robust, this model can be inadequate in cases of mixed fiber presence or more complex orientations, and so to handle more complex diffusion patterns, various alternatives have been introduced: weighted mixtures [1,2,3,4,5], higher order tensors [6], and directional functions [7]. In contrast, nonparametric techniques estimate a fiber orientation distribution function (fODF) describing an arbitrary configuration of fibers. For this estimation, several techniques have been proposed, among them Q-ball [2], spherical harmonics [8,9], spherical deconvolution [10,11,12,7], reconstruction with constant solid angle [13], and diffusion orientation transform [14].

All of those methods rely on different techniques for reconstructing, and regulazing the pathways. Deterministic tractography using the single tensor model simply follows

the principal diffusion direction, whereas multi-fiber models use various techniques for determining the number of fibers present. While parametric methods directly describe the principal diffusion directions, interpreting the fODFs from model independent representations typically involves a separate algorithm to determine the number and orientation of diffusion patterns present [15,10,9,16,17].

1.1 Our Contributions

In this study we propose a single unified optimization framework for estimating the parameters of any diffusion model. We place some of the most commonly used models into an Unscented Kalman Filter (UKF) framework as described in [18]. While the method in [18] used only the one and two-tensor models, we propose to extend it to the case of nonparametric models, such as spherical harmonics. The UKF framework has the advantage of estimating the model parameters and performing tractography simultaneously, resulting in an inherent regularization of the tracts at the same time. We compare several different diffusion models on clinical in-vivo scans on two very well studied fiber bundles: The tract that connects the anterior limb of the internal capsule to certain areas of the frontal lobe, and the fibers connecting the thalamus to the cortical regions. Furthermore, we propose two new measures for in-vivo comparison of fiber tracts resulting from different tractography techniques.

2 Methods

In Section 2.1 we describe the different models compared in this paper. Section 2.2 outlines how the models can be put into state space form and how an unscented Kalman filter can be used for estimation of the model parameters while performing tractography.

2.1 Fiber Representations

We chose a total of seven diffusion representation models to investigate in detail. Four parametric mixture models, and three nonparametric techniques.

Each representation strives to consolidate a diffusion signal $\mathbf{s} = [s_1, \ldots, s_n]^T \in \mathbb{R}^n$, measured along the corresponding gradients, $\mathbf{q}_1, \ldots, \mathbf{q}_n \in \mathbb{S}^2$ (on the unit sphere), with the underlying model. The parametric models studied in this work, are all based on the general formulation of a mixture of Gaussian tensors,

$$s(\mathbf{q}_i) = s_0 \sum_j w_j e^{-b\mathbf{q}_i^T D_j \mathbf{q}_i}, \tag{1}$$

where s_0 is a baseline signal intensity, b is an acquisition-specific constant, w_j are convex weights, and D_j is a tensor matrix describing a diffusion pattern. From this general mixture model, we derive four specific representations of the diffusion pattern.

In the simplest case, we assume only one tensor component of ellipsoidal shape (1T), i.e., one principal diffusion direction $\mathbf{m}$ with eigenvalue λ_1 and the remaining orthonormal directions have equal eigenvalues $\lambda_2 = \lambda_3$ (as in [4,19,7]).

It has been suggested that tractography may be improved in some cases by modeling the diffusion properties of free water separately from the diffusion in brain tissue [5]. Under the assumption that the free water is unrestricted by microstructural barriers, it can be modeled by a diagonal isotropic tensor D_{iso} with just one eigenvalue $\lambda_{iso} = 3 \cdot 10^{-3} mm^2/s$, the apparent diffusion coefficient of free water at body temperature. Consequently, the 1T model can be extended into a mixture of an ellipsoidal component

modeling the diffusion along axons, and an isotropic component modeling the diffusion of free water:

$$s(\mathbf{q}_i) = s_0 \left(w_1 e^{-b\mathbf{q}_i^T D \mathbf{q}_i} + w_2 e^{-b\mathbf{q}_i^T D_{iso} \mathbf{q}_i} \right).$$

This will be called the one tensor model with free water estimation (1T-FW).

In the presence of fiber crossings the single tensor models may perform poorly, as they are unable to pick up the second fiber direction [20,18]. One can extend the 1T, and 1T-FW models by adding an additional ellipsoidal diffusion tensor to each , giving the two-tensor (2T):

$$s(\mathbf{q}_i) = \frac{s_0}{2} e^{-b\mathbf{q}_i^T D_1 \mathbf{q}_i} + \frac{s_0}{2} e^{-b\mathbf{q}_i^T D_2 \mathbf{q}_i},$$

and the two-tensor model with free water estimation (2T-FW)

$$s(\mathbf{q}_i) = s_0 \left(\frac{w_1}{2} e^{-b\mathbf{q}_i^T D_1 \mathbf{q}_i} + \frac{w_1}{2} e^{-b\mathbf{q}_i^T D_2 \mathbf{q}_i} + w_2 e^{-b\mathbf{q}_i^T D_{iso} \mathbf{q}_i} \right).$$

Note, that for the last two cases the ellipsoidal tensors are equally weighted. This is justified by the fact, that the eigenvalues of the ellipsoidal tensors adjust to fit the signal in much the same way a fully weighted model would adjust.

Instead of making prior assumptions regarding the shape of the signal, it is possible to estimate the diffusion orientation density function (dODF) or the underlying fiber orientation density function (fODF), directly from the signal. This has the advantage that any number of fibers can be estimated without prior knowledge. However, the principal diffusion direction(s) are not inherently available, but must be extracted from the fODF. Such an approach was taken in [9], where the dODF is first estimated followed by a "sharpening transform" to obtain the fODF. We will call this method the "sharpened spherical harmonics" or simply spherical harmonics (SH).

Spherical deconvolution (SD) as described in [12,21] (i.e., filtered spherical deconvolution) makes the assumption that the diffusion characteristics of all fiber populations found in the brain are identical in everything but orientation. Based on this, the signal can be expressed as the convolution on the unit sphere between the fODF and a single fiber response function that can be estimated from the data itself. The fODF can then be found through a spherical deconvolution. This calculation is reduced to a simple matrix inversion when the signal is represented in a spherical harmonics basis,

$$s(\mathbf{q}_i) = \sum_{j=0}^{R} c_j Y_j(\mathbf{q}_i), \tag{2}$$

where $Y_j(\cdot)$ is the modified symmetric, real and orthonormal spherical harmonics basis, and c_j are its coefficients [22,12].

Another method to deblur the dODF was proposed by [13]. The infinitesimal element of the dODF was rewritten to cover a cone of constant solid angle, as opposed to a cylindrical shape as was done in [9,22,20]. This takes into account the quadratic growth of the volume element with respect to its distance from the origin. By following through the calculations the relation of the dODF to the signal is derived as, $dODF(\mathbf{q}_i) = \frac{1}{4\pi} + \frac{1}{16\pi^2} FRT \left\{ \nabla_b^2 \ln(-\ln s(\mathbf{q}_i)) \right\}$, where ∇_b^2 is the Laplace-Beltrami operator and FRT is the Funk-Radon Transform. This method directly estimates the fODF from the signal. We will call this method "solid angle" spherical harmonics (SA).

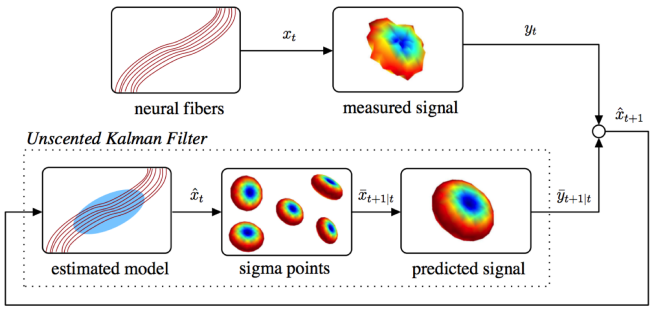

Fig. 1: System overview illustrating relation between the neural fibers, the scanner signals, and the unscented Kalman filter as it is used to estimate the local model. At each step, the filter uses its current model state to reconstruct a synthetic signal and then compares that against the actual signal from the scanner in order to update its internal model state.

2.2 Estimating the Fiber Model

In order to estimate the models described in the last section we chose the Unscented Kalman Filtering approach described in our earlier work [18]. As opposed to the the classical linear Kalman filter, the UKF can perform nonlinear estimation as is needed for the highly nonlinear reconstruction of the signals (for the parametric models).

Given the measured scanner signal at a particular voxel, we want to estimate the underlying model parameters that explain this signal. At each step, we examine the measured signal at that position, estimate the underlying model parameters, and propagate forward in the most consistent direction, i.e. the component direction most aligned with the incoming vector. Recursive estimation in this manner greatly improves the accuracy of resolving individual orientations and yields inherently smooth tracts despite the presence of noise and uncertainty. Fig. 1 illustrates this filtering process. In principal, any model can be estimated in this manner.

In order to put the studied models into state-space form, we need to define four filter components for each: 1) The system state $\mathbf{x}$: the model parameters, 2) The state transition $f[\cdot]$: how the model changes as we trace the fiber, 3) The observation $h[\cdot]$: how the signal appears given a particular state, 4) The measurement $\mathbf{y}$: the actual signal obtained from the scanner.

For all models we assume the state transition $f[\cdot]$ to be identity, which reflects the assumption, that the local fiber configuration does not undergo drastic change from one position to the next. Furthermore, the observation $h[\cdot]$ is simply the reconstruction of, $\mathbf{y} = \mathbf{s} = [s_1, \ldots, s_n]^T$, where $\mathbf{s}$ is given by the respective models for the nonparametric models, and the spherical harmonics reconstruction given in Eq. 2 for the nonparametric models.

For the two diffusion tensor based models with free water estimation (1T, 2T) the state consists of the principal diffusion direction $\mathbf{m}$ and the major and minor eigenvalues λ_1, λ_2 of each tensor. For the free water cases (1T-FW, 2T-FW), additionally the state is augmented by the weight w_1. Note, that it is not necessary to include w_2 since the weights are convex, and consequently $w_2 = 1 - w_1$. The state for the spherical harmonics based methods is the vector of coeffficients c_j in the SH basis (see Eq. 2).

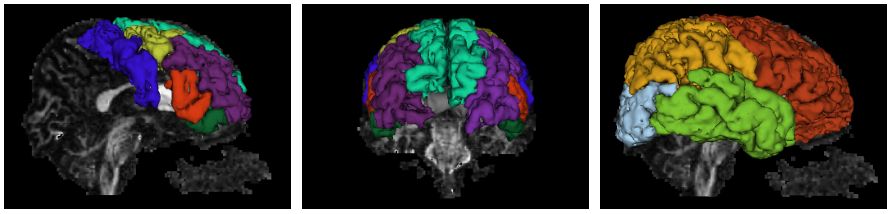

Fig. 2: Left and Middle (a): R-L and A-P view of the desired and undesired connectivity regions for fibers passing through the anterior limb of the internal capsule (white). Desired: superior-frontal gyrus (turquoise), rostral-middle-frontal gyrus (purple), pars-trianglaris (red), and pars-orbitalis (green). Undesired: precentral gyrus (blue), and caudal-middle-frontal gyrus (yellow). **Right (b)**: The 4 lobes: frontal (red), temporal (green), parietal (yellow), and occipital lobe (blue).

3 Experiments

The seven diffusion models from Section 2.1 were compared on brain scans of 10 healthy human subjects. The images were acquired using a 3-Tesla magnet and 51 distinct diffusion gradient directions at $b = 900 s/mm^2$.

We assessed the quality of the tractography for each method based on two very well studied fiber tracts. First, we investigated the fibers that travel through the anterior limb of the internal capsule to certain areas of the frontal lobe. This connectivity is known from postmortem and histology studies [23]. Based on information provided to us by an expert neuroanatomist the fiber bundle should pass through the anterior limb of the internal capsule and connect to the superior-frontal gyrus, rostral-middle-frontal gyrus, pars trianglaris, and the pars orbitalis. Furthermore, the **fibers do not connect** to the adjoining areas of precentral gyrus, and the caudal-middle-frontal gyrus (see Fig. 2a).

Secondly, we investigated the thalamo-cortical connections as described in [24]. The thalamus is connected to all the four lobes of the brain and a good tractography method should be able to trace these connections (see Fig. 2b for the 4 lobes). The segmentation of the internal capsule was obtained as defined in [25] whereas the cortical segmentations were obtained with Freesurfer.

The quality of the tractography of the first fiber bundle was assessed using two novel measures (Eq. 3). The traceability $\mathcal{T}$, measures the proportion of the fibers in a bundle that go to the desired region. A fiber was counted as N_{pos} if it passed through, or ended in one of the desired regions. If it went through one of the undesired regions it was counted as N_{neg}. Note, that the measure becomes negative for a case where the number of fibers connecting to an undesired region is larger than the number of correct fibers.

The second measure, coverage $\mathcal{C}$, is given by the ratio of voxels in the target region passed by a fiber V_{fiber}, to the toal number of voxels in the target region V_{target}. While the traceability will assign a high score to fibers that go straight to one region without branching, the coverage will assign a high score only to fibers that cover a large area of the target region, which is expected from the anatomy.

$$\mathcal{T} = \frac{N_{pos} - N_{neg}}{N_{total}}, \qquad \mathcal{C} = \frac{V_{fiber}}{V_{target}} \tag{3}$$

To generate the fiber tracts we began by seeding each voxel once, and traced the fibers for each of the diffusion models until the anisotropy threshold was reached. We

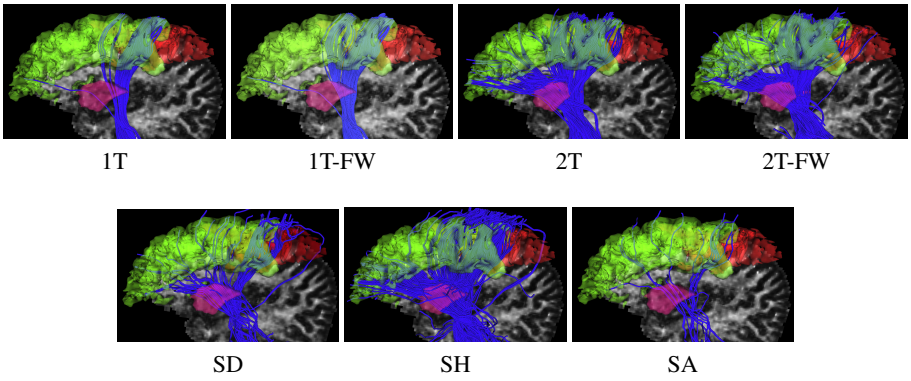

Fig. 3: Fiber bundles passing through the anterior limb of the internal capsule (purple) to the target region (green), and the non-target region (red) for each of the 7 examined methods.

implemented each method by closely following the corresponding papers (albeit in the UKF framework). For SH, and SD, we chose the order of the spherical harmonics $L = 6$, for SA we set $L = 4$. The peak extraction of the respective ODFs was performed following the method described in [26].

From the resulting tractography of each hemisphere, we extracted the fibers that pass through the anterior limb of the internal capsule, or the thalamus. These filtered fiber sets served as starting point to calculate the scores described above.

The resulting fibers for the tract through the internal capsule are shown in Fig. 3. The tracability and coverage scores for this tract are shown in Fig. 4. The percentage per lobe, and the coverage of the fibers passing through the thalamus are shown in Fig. 4. The coloring of the bars corresponds to the lobes in Fig. 2b.

Anterior Internal capsule results: From the results, it is clear that, while the 1T and 1T-FW methods get the best score for traceability, they perform very poorly in coverage $\mathcal{C}$ (as can be seen in Fig. 2a). Thus, these methods have little false positives but they do not connect to all parts of the target regions (as is known from human anatomy). The 2T, 2T-FW and SH methods perform well in both measures $\mathcal{T}$, and $\mathcal{C}$. However, the method 2T-FW seems to perform the best, providing a nice balance between traceability and coverage.

Thalamo-cortical results: For this fiber bundle, the results demonstrate that the parametric models (2T, 2T-FW) perform significantly better in terms of connecting all the different lobes of the brain compared to the nonparametric methods. Thus, while all methods find the thalamo-cortical connections to each of the lobes, the coverage of the 2T and 2T-FW is significantly better. This is in tune with known anatomical results and using the probabilistic tractography method of [24].

4 Discussion and Conclusions

In this work, we proposed the UKF framework to estimate several parametric and non-parametric diffusion models and subsequently compared their ability to trace two known fiber bundles in the human brain. The comparison in this work truly demonstrates the differences in each model since the optimization framework is the same for

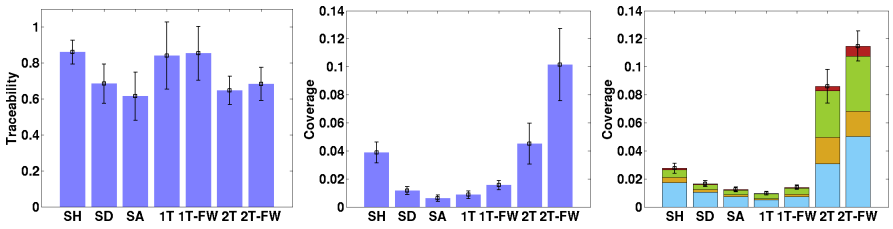

Fig. 4: Left and Middle: Resulting scores for traceabilty and coverage for the fiber bundle passing through the anterior limb of the internal capsule. **Right**: Coverage of the fibers passing through the thalamus. The colors correspond to the lobes outlined in Fig. 2b. All scores are averaged over 10 subjects.

all the models. We should also note that, there has been a lot of work in the literature on comparing individual models, either using Monte-Carlo simulations at a single voxel level or on a diffusion phantom (Fiber cup) or on in-vivo data as in [27]. However, in this work we propose to perform comparison using the same optimization framework for all diffusion models and compare the ability of each of these methods to trace the fiber bundle of interest (connectivity known from the anatomy) on a clinical scan.

While, the one tensor methods are significantly better in terms of traceability, however, they perform poorly in terms of coverage of the target region. On the other hand the sharpened spherical harmonics, and the two 2-Tensor methods (2T, 2T-FW) perform very well in terms of coverage for both the fiber bundles. For the fibers passing through the thalamus, the 2T-FW method outperform all other methods, in term of coverage. Furthermore, the 2-Tensor methods find some fibers in the frontal, and parietal lobe, where the other methods find almost none. We should note that, the proposed work is by no means an exhaustive comparison of the different models, however, it does provide a way to compare the various diffusion models proposed in the literature in a single optimization framework. Further, the results shown in this work are for a particularly low b-value ($b = 900\ s/mm^2$). It is expected that the methods like SA and SD will perform significantly better at higher b-values.

References

1. Alexander, A., Hasan, K., Tsuruda, J., Parker, D.: Analysis of partial volume effects in diffusion-tensor MRI. Magnetic Resonance in Medicine **45** (2001) 770–780
2. Tuch, D., Reese, T., Wiegell, M., Makris, N., Belliveau, J., Wedeen, V.: High angular resolution diffusion imaging reveals intravoxel white matter fiber heterogeneity. Magnetic Resonance in Medicine **48** (2002) 577–582
3. Kreher, B., Schneider, J., Mader, I., Martin, E., Hennig, J., Il'yasov, K.: Multitensor approach for analysis and tracking of complex fiber configurations. Magnetic Resonance in Medicine **54** (2005) 1216–1225
4. Parker, G., Alexander, D.C.: Probabilistic anatomical connectivity derived from the microscopic persistent angular structure of cerebral tissue. Phil. Trans. R. Soc. B **360** (2005) 893–902
5. Pasternak, O., Sochen, N., Gur, Y., Intrator, N., Assaf, Y.: Free water elimination and mapping from diffusion mri. Magnetic Resonance in Medicine **62**(3) (2009) 717–730
6. Basser, P.J., Pajevic, S.: Spectral decomposition of a 4^{th}-order covariance tensor: Applications to diffusion tensor MRI. Signal Processing **87** (2007) 220–236

7. Kaden, E., Knøsche, T., Anwander, A.: Parametric spherical deconvolution: Inferring anatomical connectivity using diffusion MR imaging. NeuroImage **37** (2007) 474–488
8. Anderson, A.: Measurement of fiber orientation distributions using high angular resolution diffusion imaging. Magnetic Resonance in Medicine **54**(5) (2005) 1194–1206
9. Descoteaux, M., Deriche, R., Anwander, A.: Deterministic and probabilistic Q-ball tractography: from diffusion to sharp fiber distributions. Technical Report 6273, INRIA (2007)
10. Jian, B., Vemuri, B.: A unified computational framework for deconvolution to reconstruct multiple fibers from diffusion weighted MRI. Trans. on Med. Imag. **26**(11) (2007) 1464–1471
11. Jansons, K., Alexander, D.C.: Persistent angular structure: New insights from diffusion MRI data. Inverse Problems **19** (2003) 1031–1046
12. Tournier, J.D., Calamante, F., Gadian, D., Connelly, A.: Direct estimation of the fiber orientation density function from diffusion-weighted MRI data using spherical deconvolution. NeuroImage **23** (2004) 1176–1185
13. Aganj, I., Lenglet, C., Sapiro, G., Yacoub, E., Ugurbil, K., Harel, N.: Reconstruction of the orientation distribution function in single-and multiple-shell q-ball imaging within constant solid angle. Magnetic Resonance in Medicine **64**(2) (2010) 554–566
14. Özarslan, E., Shepherd, T., Vemuri, B., Blackband, S., Mareci, T.: Resolution of complex tissue microarchitecture using the diffusion orientation transform. NeuroImage **31**(3) (2006) 1086–1103
15. Zhan, W., Yang, Y.: How accurately can the diffusion profiles indicate multiple fiber orientations? A study on general fiber crossings in diffusion MRI. J. of Magnetic Resonance **183** (2006) 193–202
16. Bloy, L., Verma, R.: On computing the underlying fiber directions from the diffusion orientation distribution function. In: Medical Image Computing and Computer Assisted Intervention (MICCAI). (2008) 1–8
17. Schultz, T., Seidel, H.: Estimating crossing fibers: A tensor decomposition approach. Trans. on Visualization and Computer Graphics **14**(6) (2008) 1635–1642
18. Malcolm, J., Shenton, M., Rathi, Y.: Filtered multitensor tractography. Medical Imaging, IEEE Transactions on **29**(9) (2010) 1664–1675
19. Friman, O., Farnebäck, G., Westin, C.F.: A Bayesian approach for stochastic white matter tractography. Trans. on Med. Imag. **25**(8) (2006) 965–978
20. Tuch, D.: Q-ball imaging. Magnetic Resonance in Medicine **52** (2004) 1358–1372
21. Tournier, J.D., Calamante, F., Connelly, A.: Robust determination of the fibre orientation distribution in diffusion MRI: Non-negativity constrained super-resolved spherical deconvolution. NeuroImage **35** (2007) 1459–1472
22. Descoteaux, M., Deriche, R., Knoesche, T., Anwander, A.: Deterministic and probabilistic tractography based on complex fiber orientation distributions. Trans. on Med. Imag. **28**(2) (2009) 269–286
23. Carpenter, M.: Core text of neuroanatomy, ed 4, baltimore, 1991
24. Behrens, T., Johansen-Berg, H., Woolrich, M., Smith, S., Wheeler-Kingshott, C., Boulby, P., Barker, G., Sillery, E., Sheehan, K., Ciccarelli, O., et al.: Non-invasive mapping of connections between human thalamus and cortex using diffusion imaging. Nature neuroscience **6**(7) (2003) 750–757
25. Mori, S., Wakana, S., Van Zijl, P., Nagae-Poetscher, L.: MRI atlas of human white matter. Am Soc Neuroradiology (2005)
26. Descoteaux, M.: High Angular Resolution Diffusion MRI: from Local Estimation to Segmentation and Tractography. PhD thesis, University of Nice-Sophia Antipolis (2008)
27. Yo, T., Anwander, A., Descoteaux, M., Fillard, P., Poupon, C., Knösche, T.: Quantifying brain connectivity: A comparative tractography study. Medical Image Computing and Computer-Assisted Intervention–MICCAI 2009 (2009) 886–893